

# A motion-sensitive neurone responds to signals from the two visual systems of the blowfly, the compound eyes and ocelli

Matthew M. Parsons<sup>1,\*</sup>, Holger G. Krapp<sup>2</sup> and Simon B. Laughlin<sup>1</sup>

<sup>1</sup>Department of Zoology, University of Cambridge, Downing Street, Cambridge, CB2 3EJ, UK and <sup>2</sup>Department of Bioengineering, Imperial College London, South Kensington Campus, London, SW7 2AZ, UK

\*Author for correspondence (e-mail: mmp26@cam.ac.uk)

Accepted 25 September 2006

## Summary

In the blowfly *Calliphora vicina*, lobula plate tangential cells (LPTCs) estimate self-motion by integrating local motion information from the compound eyes. Each LPTC is sensitive to a particular (preferred) rotation of the fly's head. The fly can also sense rotation using its three ocelli (simple eyes), by comparing the light intensities measured at each ocellus. We report that an individually identified tangential cell, V1, responds in an apparently rotation-specific manner to stimulation of the ocelli. This effect was seen with or without additional stimulation of the compound eye. We delivered stimuli to the ocelli which mimicked rotation of the fly's head close to that of the preferred axis of rotation of V1. Alternating between

preferred and anti-preferred rotation elicited a strongly phasic response, the amplitude of which increased with the rate of change of light intensity at the ocelli. With combined stimulation of one compound eye and the ocelli, V1 displayed a robust response to ocellar stimuli over its entire response range. These findings provide the opportunity to study quantitatively the interactions of two different visual mechanisms which both encode the same variable – the animal's rotation in space.

Key words: ocelli, compound eye, vision, tangential cell, LPTC, blowfly, *Calliphora*, invertebrate, multisensory integration, electrophysiology, neural processing.

## Introduction

Most flying insects have a rather limited range of behavioural goals during flight. Besides 'higher order' behaviours such as courtship and territorial maintenance, the basic pre-requisites for successful flight are simply stability, and collision avoidance. Of these two, stability is the more interesting in terms of multi-sensory integration, because it requires contributions from many of the insect's wide range of sensory systems (Hengstenberg, 1993; Sherman and Dickinson, 2003).

Each modality has inherent, unavoidable physical or neural limitations that restrict its effectiveness as the sole sensor for a particular type of in-flight stimulus (Hengstenberg, 1993; Keil, 1997; Krapp and Hengstenberg, 1996; Nalbach, 1993). Complementary sensory modalities can be very important, to cover a large dynamic range and therefore provide adequate information on flight perturbations. For instance, in the fly visual system, self-rotations are estimated by integrating the outputs of many elementary motion detectors (EMDs). EMDs receive their inputs from the compound eye and locally analyse directional motion. However, because an EMD, or Reichardt Correlator (Haag et al., 2004; Reichardt, 1987), is a delay-based directionally selective mechanism, it requires extra processing time, and this limits self-motion estimation to a

range of comparatively low angular velocities. To maintain flight and gaze stability in the higher angular velocity range, flies make use of information from other sensory systems including mechanoreceptors on the halteres (Fraenkel and Pringle, 1938; Nalbach, 1993; Nalbach and Hengstenberg, 1994) and the wings (Fayyazuddin and Dickinson, 1999; Heide, 1974), and the photoreceptor-based ocelli.

The ocelli (simple eyes) of the fly are a set of three small single-lens eyes which, by their construction, are well adapted to the task of rotation detection in the manner of an artificial horizon (Schuppe and Hengstenberg, 1993; Stange et al., 2002; Taylor, 1981a; Taylor, 1981b; Wilson, 1978a). By having a retina that is attached to the rear surface of the lens, the images at the level of the photoreceptors are highly blurred, i.e. they are composed only of very low spatial frequencies. It is believed that the ocelli do not make use of the remaining image structure and are only concerned with integrating light over their entire visual fields. Only for the dragonfly median ocellus is there evidence that the ocelli utilise image structure (Stange et al., 2002), based partially on anatomical adaptations of the ocellus – an enlarged, astigmatic lens and an effective 'lens hood', which are not present in flies. The ocelli are very effective rotation detectors, crucial to proper gaze and flight stabilisation in dragonflies (Stange, 1981; Stange and Howard,

1979) as well as in locusts (Taylor, 1981a; Taylor, 1981b). Ocellar contributions to gaze stabilisation have also been shown in the fly (Schuppe and Hengstenberg, 1993).

The neural processing required for an ocellar-based rotation detector is relatively simple, at least compared to the processing required for the directional motion analysis of compound eye inputs. Ocellar second-order interneurons (L-neurons) integrate the outputs of photoreceptors and code light intensity information as graded potentials (Simmons, 1999; Simmons et al., 1994; Wilson, 1978b). Although the neural mechanism by which ocellar rotation detection is implemented is unknown, one possible means of investigating this would be to directly compare the outputs of L-neurons. L-neurons also have some of the largest diameter axons in the fly nervous system (Nässel and Hagberg, 1985; Simmons et al., 1994), which allow for fast signal propagation. It is these functional adaptations of the ocellar system that facilitate fast motor responses; in the locust, the ocelli are known to elicit compensatory head movements twice as fast as the compound eyes (Taylor, 1981a). However, although a rapid response is desirable, motor responses elicited by the ocelli may in general be quite jerky in comparison to those mediated by the compound eyes, as has been observed in dragonfly (Taylor, 1981a). The integration of compound eye and ocellar outputs can realize a visual detection of rotations that combines high speed with high precision. How and where does such integration occur in the nervous system of the fly?

As mentioned above, the fly visual system contains a class of interneurons that are matched filters for particular self-motions (Krapp, 2000; Krapp et al., 1998). In the third visual neuropile of each half of the brain there are about 50 lobula plate tangential cells (LPTCs). Many of them make direct synaptic connections with descending neurons, which then convey sensory information to the various motor systems. The neuroanatomy of ocellar L-neurons is also suggestive of synapses with both LPTCs and descending neurons (Strausfeld, 1976; Strausfeld and Bassemir, 1985). Intracellular staining has shown that the terminal arborisations of ocellar L-neurons and some VS neurons overlap with the dendritic fields of descending neurons. It is known that descending neurons respond to stimuli of different modalities (Strausfeld and Gronenberg, 1990) but that the responses are quite complex, and this complicates the electrophysiological analysis of multi-modal convergence. To fully characterise the interactions of multiple modalities at a neuronal level, it is necessary to be able to deconvolve the mixed responses of individual cells.

Here we show that the activity of the well-studied tangential cell V1 (e.g. Hausen, 1993) is driven by illumination of the lateral ocelli. V1 was previously thought to be dedicated solely to processing visual information from the compound eyes. Our results suggest that V1 encodes a single, self-motion-related variable that is independently sensed by two separate sensory systems, the compound eyes and the ocelli. This discovery raises the possibility of a quantitative study of the interactions between signals from the ocelli and the compound eyes by monitoring the response of the identified V1 cell.

## Materials and methods

### Preparation

Specimens of *Calliphora vicina* Robinson-Desvoidy were taken from a culture in the Department of Zoology, Cambridge, UK. Only female blowflies were used, because the larger gap between the compound eyes on the dorsal side of the head capsule allows easier access to the ocellar nerve.

The legs, wings and proboscis of the fly were removed, and the wounds waxed shut. The fly was mounted on a custom-built copper/plastic holder. The head of the fly was aligned with the horizontal and vertical planes by using the deep pseudopupil (Franceschini, 1975). The thorax and abdomen were bent ventrally by approximately 20° to gain access to the rear of the head capsule. The cuticle of the right rear head capsule was cut open and the air sacs were moved aside to expose the lobula plate (Fig. 1). A silver wire reference electrode was inserted into a small hole in the left rear head capsule.

In experiments where the ocellar nerve was to be cauterised, the cuticle of the medial rear head capsule between the neck and the ocelli was cut away to expose the ocellar nerve. Cauterisation was performed by inserting a fine loop of tungsten wire into the exposed air cavity containing the ocellar nerve, and passing enough current through the wire to irreversibly dehydrate, but not burn, the nerve. A photograph and a schematic of the preparation are shown in Fig. 1.

### Stimulus

Stimuli to the lateral ocelli were delivered via a pair of 62.5 µm diameter glass optical fibres, such that the light output of each fibre covered only the lens of one ocellus (ocellar diameter ~100 µm) plus a minimum area of cuticle surrounding it (Fig. 1A). The fibres were connected to a pair of blue LEDs, the intensity of which was controlled by the analogue outputs of a data acquisition card (NI-6025E) at an update-rate of 5 kHz. The wavelength of the LEDs ( $\lambda_{\text{max}}=470$  nm) was sufficiently well matched to the absorption spectrum of the ocellar photoreceptor pigment (Kirschfeld et al., 1988) and was identical to that used in a previous study of fly L-neurone responses to light stimulus (Simmons et al., 1994). The output intensities of the fibres were calibrated and normalised with each other using a photoresistor.

The maximum intensity deliverable by our optical fibres was defined as  $I_{\text{max}}$ , and we chose our stimulus parameter to be intensity difference, where LED intensity difference,  $DI=(\text{Left LED output}-\text{Right LED output})$ . Our ocellar stimuli could therefore vary from  $I_{\text{max}}$  (maximum intensity at the left ocellus, zero at the right) to  $-I_{\text{max}}$  (maximum intensity at the right ocellus, zero at the left).

We used a CRT monitor to present pattern motion stimuli to the compound eyes. The monitor was driven by a dedicated visual stimulus card (Cambridge Research Systems 2/5), which operated at a refresh rate of 180 Hz. Compound eye stimuli consisted of a horizontal grating moving vertically downwards. The spatial intensity distribution of the grating was sinusoidal. To adjust the strength of the stimuli, we adjusted the contrast of the grating, rather than the velocity.

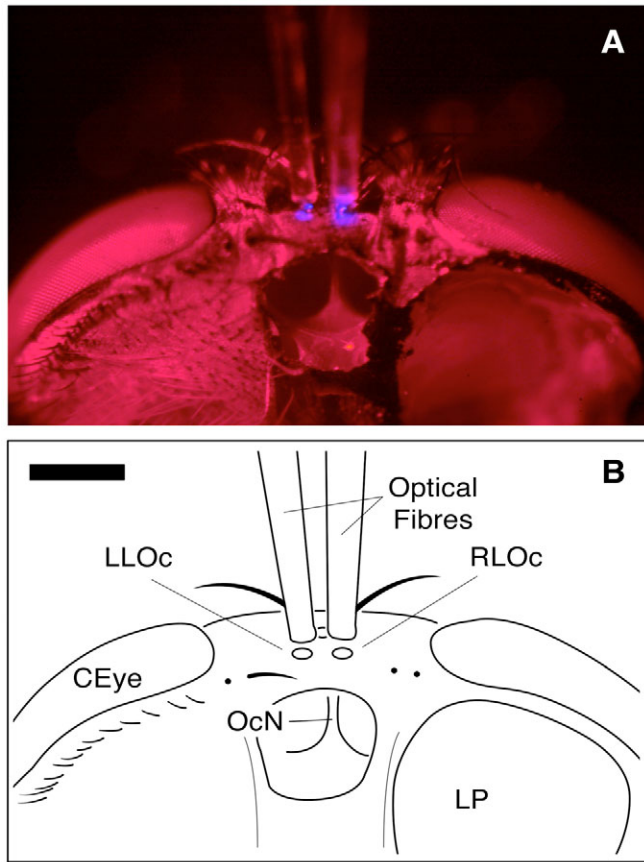


Fig. 1. Photograph (A) and line drawing (B) of the rear aspect of the head capsule of *Calliphora vicina*. Because the ends of the two optical fibres almost touch the lateral ocelli, their light outputs (blue circles in A) do not overlap. The cuticle of the posterior face of the head capsule is cut away to expose the right-hand lobula plate, and the midbrain cavity, in which the ocellar nerve connects the ocellar neuropil with the brain. Scale bar, 500  $\mu\text{m}$ . CEye, compound eye; LLOc, left lateral ocellus; RLOc, right lateral ocellus; OcN, ocellar nerve; LP, lobula plate.

In this way, the ocelli would see no overall change in brightness during compound eye stimulation. The grating was moved at a fixed contrast frequency of 5 Hz, with a spatial wavelength of 8°, across a display window of approximately 90° azimuth by 70° elevation.

#### Recordings

We recorded extracellularly from V1 using tungsten electrodes (manufacturer: FHC) with an input resistance of  $3 \pm 0.6 \text{ M}\Omega$ . The extracellular neuronal signal was band-pass filtered (0.3–5 kHz), amplified, and then sampled by a data acquisition card (AM Systems 1700 differential AC and National Instruments 6025E, respectively) at a sample rate of 40 kHz onto the hard-drive of a computer running Windows XP.

#### Cell identification and receptive field characteristics

In order to identify V1 recordings, the centre of the CRT was positioned at an azimuth of  $-45^\circ$  and an elevation of  $0^\circ$  (grey

area in Fig. 2) relative to the reference frame of the fly head capsule, where  $0^\circ$  azimuth,  $0^\circ$  elevation means the point directly in front of the fly. In this region of its receptive field, V1 is most strongly excited/inhibited by downward/upward motion (Krapp et al., 2001) (Fig. 2). V1 can be easily distinguished from the other spiking LPTCs sensitive to vertical motion in the equatorial visual field, i.e. V2 and Vx. V2 is excited by pattern motion in the opposite direction (upwards), and Vx in this area responds, but is much less sensitive to, vertical downward motion (Krapp, 1995).

#### Data analysis

We obtained recordings from 10 blowflies at signal-to-noise ratios that allowed us to reliably separate V1 spikes. In Fig. 3, V1 activity is given in terms of instantaneous spike rate (ISR). However, the resolution of averaged instantaneous spike rate data is limited by the average spike rate of the cell and the number of repetitions of a stimulus protocol. For our data, the instantaneous spike rate does not properly represent inhibition on short time scales, or the timing of individual spikes. Therefore, in the rest of the paper, the spike rate,  $R(t)$ , of the cell is expressed as normalised, averaged Gaussian-convolved spike trains (Gabbiani et al., 1999):

$$R(t) = \rho(t) * g(x) = \left( \sum_i^N \delta(t-t_i) \right) * \left( \frac{1}{\alpha\sqrt{2\pi}} e^{-x^2/2\sigma^2} \right), \quad (1)$$

Here,  $R(t)$  is formed from the convolution of  $\rho(t)$ , a train of  $N$  spikes as represented by a sum of delta functions at times  $t_i$ , with  $g(x)$ , a Gaussian with full-width at half-maximum (FWHM) of  $\sim 2.35\sigma$ .  $R(t)$  was then normalised so that the integral of the entire function was equal to the total number of spikes comprising the original spike train:

$$\hat{R}(t) = R(t) \times \frac{N}{\int_0^T R(t) dt}. \quad (2)$$

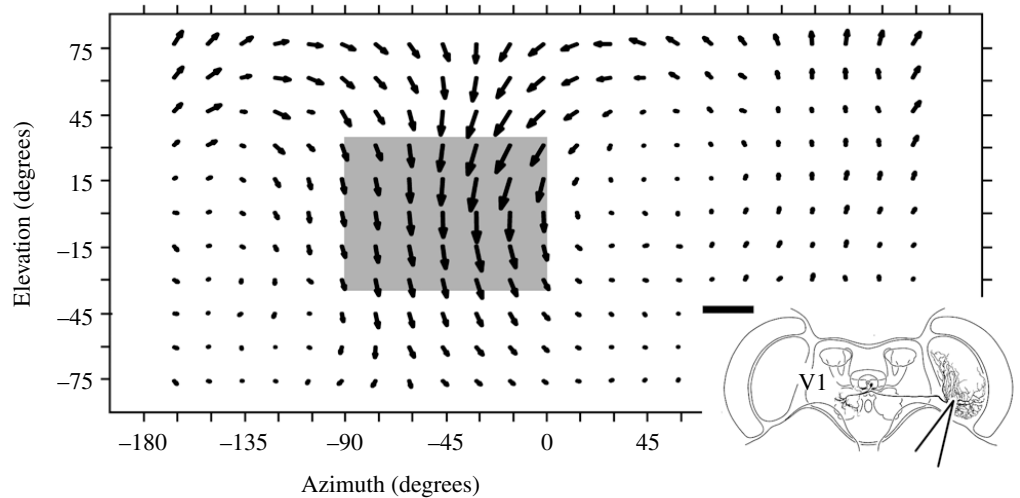
$R(t)$  is referred to in the rest of the text as instantaneous firing rate. The FWHM of our smoothing function was always set as 5 ms. Errors on averaged data are always given as standard error of the mean ( $\pm 1$  s.e.m.) and are shown as white or shaded areas around the averaged data. Fits to the data in the last figure were obtained using the Matlab Data Fitting Toolbox, using a smoothing spline.

## Results

### V1 responds to stimulation of the lateral ocelli

Once a stable extracellular recording was established in V1, we presented stimuli to the lateral ocelli that mimicked roll rotations of the head. V1 responded consistently to step changes in illumination of the left and right lateral ocelli. Transient excitation of V1 was seen subsequent to a switch in illumination from the right to left ocellus – a fictive clockwise roll. An extended period of inhibition of V1 followed a switch

Fig. 2. The receptive field organisation and morphology of the V1 neurone [receptive field modified from Krapp et al. (Krapp et al., 2001)]. The orientation and length of each arrow in the vector map indicates the local directional motion preference and sensitivity, respectively. The map resembles the optic flow pattern generated by a rotation of the head about an axis approximately midway between pitch and roll (nodes at  $\sim 45^\circ$  and  $\sim -135^\circ$  azimuth). The grey box shows the approximate area and position of the display monitor we used for stimulating the compound eye. Inset: A schematic drawing of the fly brain, with a camera lucida drawing of a stained V1 neurone on the right-hand side (courtesy of Klaus Hausen). The approximate electrode position is indicated by the open arrowhead. Scale bar,  $200\ \mu\text{m}$ .



from the left to right ocellus – a fictive anticlockwise roll (Fig. 3A,B).

To confirm that this effect is ocellar-mediated, we performed two control experiments. It was possible, though unlikely, that the unshielded compound eyes could see LED light reflected from surrounding objects, and that this was changing the spike rate in V1. We eliminated this possibility by moving the light guides from their positions above the lateral ocelli to a nearby piece of opaque cuticle, and then repeating the experiment. This extinguished the response of V1 to the LED stimuli. We were also able to discount the other possible explanation for the effect, i.e. that light was transmitted through the ocelli, the transparent tissue of the brain, and into the compound eye photoreceptors. We left the light guides in their positions above the lateral ocelli, and then cauterised the ocellar nerve by passing current through a small wire loop (see Materials and methods). The response of V1 to changes in illumination of the lateral ocelli was again extinguished (Fig. 3C). These controls demonstrate that V1 is driven by the ocelli.

Finally, to make sure that V1 had not been damaged during cauterisation, we tested the cell's response to directional motion stimuli displayed to the compound eyes before and after cauterisation. We found that the response of V1 to a moving grating (Fig. 3E, time course of grating contrast) after cauterisation (Fig. 3F) was very similar to the response before (Fig. 3D); the datasets prior to and after cauterisation lie within each other's error bounds (cf. coloured lines in Fig. 3D,F). These results show that cauterising the ocellar nerve did not impair the spiking activity of V1.

#### *V1 spikes are phase-locked to ocellar stimuli*

Using the same stimulus procedure as described above (Fig. 3), we repetitively stimulated the ocelli with trains of step changes in light intensity, and calculated instantaneous firing rate (see Materials and methods) and spike time histograms. Repetitions of the stimulus trains were separated by 2.5 s

intervals. In these experiments, V1 displayed marked phase-locking of spikes, along with clear periods of complete inhibition (Fig. 4A,B). The highest temporal coherence was only seen for the first spike following excitatory stimuli, hence the vertical lines seen in the spike raster plot (Fig. 4B). At the stimulus frequency shown here (10 Hz) the temporal coherence of the phase-locked spikes slightly decayed with each stimulus cycle (cf. Fig. 4A, peaks of the grey top trace). The standard deviation of the spike position, or 'spike jitter', for this cell was 0.3 ms for the 1st cycle, decaying to 3 ms for the 15th cycle. The mean for the 1st and 15th stimulus cycle of 10 animals was  $\sim 4$  ms and  $\sim 11$  ms, respectively. The decay in temporal coherence appears to halt after  $\sim 500$  ms of stimulation (Fig. 4A).

#### *V1 responses to ocellar stimuli are phasic*

Ocellar L-neurons display rapid, transient changes in membrane potential in response to stimulation of the ocelli (Simmons et al., 1994), and this should be reflected in the responses of downstream neurones. We recorded the activity of V1 in response to light intensity steps and to sinusoidal changes in light intensity, for the purpose of qualitative comparison to L-neurone responses. As before, stimuli were applied in near darkness.

For excitatory stimuli, both step (Fig. 5B) and sinusoidal (Fig. 5D) excitatory stimuli elicited the characteristic phasic-tonic response shape of L-neurone responses to changes in light intensity (Fig. 5A,C). For inhibitory stimuli, any phasic inhibition of V1 was masked by the low spontaneous spike rate of the cell. The peak instantaneous firing rate during the sinusoidal stimulus (Fig. 5C) was considerably smaller than that elicited by the step stimulus. This observation suggests that, as in ocellar L-neurons, the peak response was related to the rate of change of light intensity at the ocelli (Simmons et al., 1994), which in turn was closely related to the velocity of head rotation.

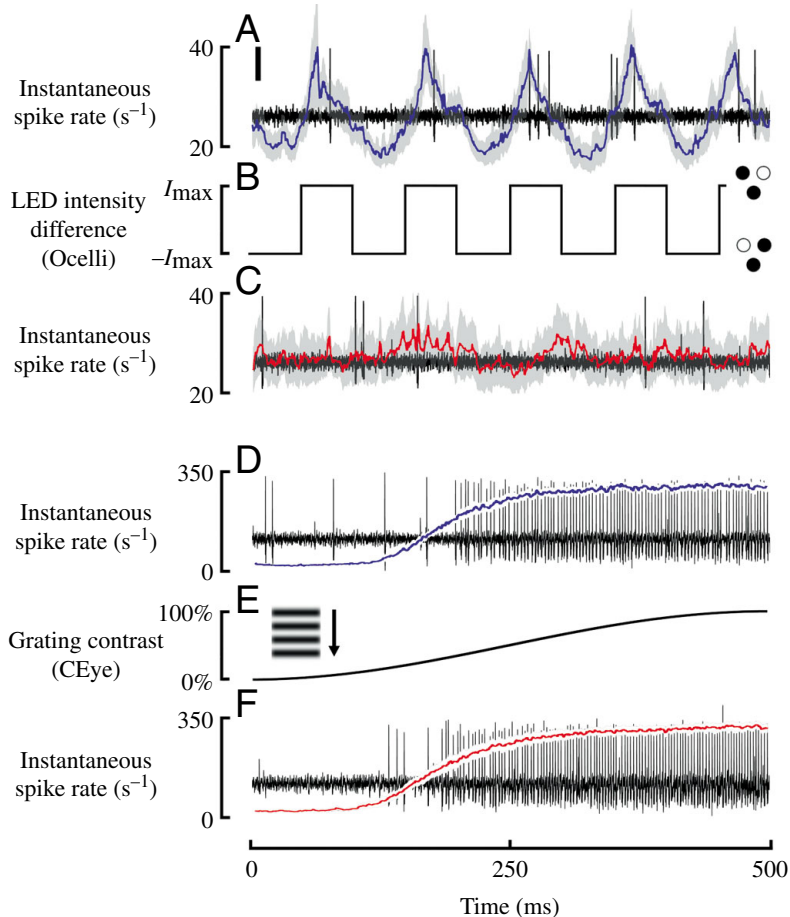


Fig. 3. The response of V1 neuron to stimulation of the ocelli (A–C) and compound eyes (D–F) before (blue curves) and after (red curves) cauterisation of the ocellar nerve. The coloured curves show instantaneous spike rates (ISRs) averaged over 563 trials, and overlay extracellular recordings of V1's spike activity during a single trial. (A) ISR and representative recording before cauterising the ocellar nerve (scale bar,  $15 \mu\text{V}$ ). The grey shading indicates variability of ISR,  $\pm 1$  s.e.m. The baseline of the extracellular recording indicates the mean spontaneous spike rate. (B) Stimulus presented to the right and left lateral ocelli. LED intensity difference = (left LED output – right LED output);  $I_{\text{max}}$ , max LED output. The dots show illumination switching between left and right ocelli as the LED intensity difference switches from  $I_{\text{max}}$  to  $-I_{\text{max}}$ . (C) Greatly reduced activity in V1 after cauterising the ocellar nerve, traces as in A. (D) ISR recorded in response to compound eye stimulation before cauterisation of the ocellar nerve. Traces as in A and C, but variability ( $\pm 1$  s.e.m.) is shown as a white band against the background of recorded spikes. (E) Compound eye stimulus: a horizontal sinusoidal grating (spatial frequency =  $0.63 \text{ cycles deg}^{-1}$ ) moving in V1's preferred direction, vertically downwards at  $40 \text{ deg. s}^{-1}$ . Grating contrast was progressively increased over each trial to drive V1 over its full range of spike rate. (F) Response to compound eye stimulus after cauterisation of the ocellar nerve. The complete set of experiments was performed with five animals, giving a total of 563 trials for each stimulus protocol.

*Latency of post-stimulus spikes in V1 is reduced by stimulation of the compound eyes*

All the characteristics of the results shown in Figs 4 and 5, such as phase-locked spiking and phasic–tonic responses were reproduced in nine more animals (Fig. 6A). In detail, however, we found considerable variability between individual responses. The amplitude and latency of the peaks (Fig. 6A) varied from 21–134 spikes  $\text{s}^{-1}$  and 10.5–29 ms, respectively. Such high inter-individual response variability is well documented for the V1 cell (e.g. Karmeier et al., 2003). The latency of the first spike, given by the time difference between stimulus onset and the peak in the instantaneous firing rate, had a median of  $\sim 16$  ms. In two recordings, however, the latencies were markedly increased to  $\sim 28$  ms. The V1 cells studied in these two experiments also differed from the other V1 cells in that they showed particularly low spontaneous activities. On a graph of latency *versus* spontaneous rate (Fig. 6C) these two points appear at the top left. This graph suggests that the latency of ocellar drive to V1 is in some way dependent on the present activity of the cell. To assess the validity of this, we measured the peak latency again, except this time the rate of V1 was raised by means of compound eye stimulation (moving grating; see Fig. 3 and Materials and methods) during ocellar stimulation. By raising the spike rate of V1 to  $>250$  spikes  $\text{s}^{-1}$  in five cells, we found that the peak latency was reduced by an

average of 4 ms, from 16 ms to 12 ms. These reduced latencies are shown in Fig. 6C as blue crosses.

*V1's ocellar response increases with the rate of change of light intensity*

After we found that V1 responds better to sudden steps than to more gradual sinusoids we measured the relationship between V1's peak response and the rate of change of light intensity in the two lateral ocelli. As in our previous experiments (e.g. Fig. 3B) we used stimuli where any change in light intensity in one ocellus was accompanied by an equal and opposite change in the other ocellus. The intensity of this symmetrical stimulus can be described as the difference between the intensities in the left and the right ocellus,  $DI = (I_L - I_R)$  and  $DI$  ranges from  $-I_{\text{max}}$  to  $I_{\text{max}}$ , where  $I_{\text{max}}$  corresponds to the maximum intensity of each of the two matched LEDs. When  $DI$  is ramped at a constant rate from  $I_{\text{max}}$  in one ocellus to  $I_{\text{max}}$  in the other, the rate of change of  $DI$  is  $2I_{\text{max}}/t$ , where  $t$  is the time it takes to complete the ramp. We recorded the response of V1 for stimuli that first ramped up and then ramped down at an equal (but opposite) rate (Fig. 7A). The ramp up corresponds to a clockwise roll ( $I_L$  is increasing) and the ramp down to an anticlockwise roll, consequently V1 is first excited by this stimulus and then inhibited (Fig. 7A). The instantaneous firing rates and spike time histograms were

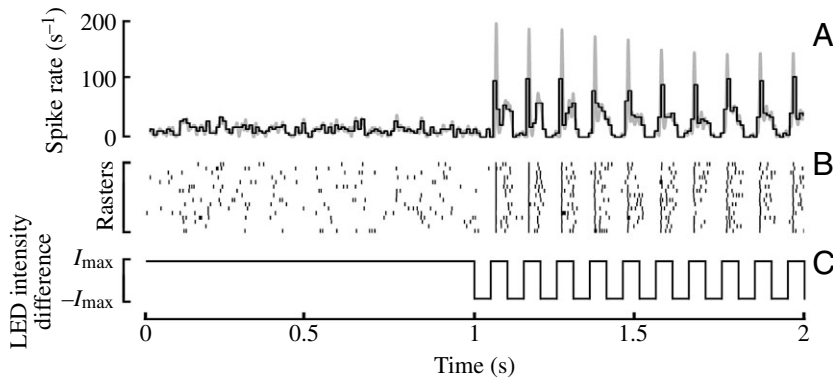


Fig. 4. Response of V1 neuron to repetitive stimulation of the lateral ocelli, showing that a switch in illumination from right to left ocellus generates a phase locked spike in V1, whose jitter increases over successive repetitions. (A) Responses averaged over 29 stimulus trials in a single animal; black line, peristimulus spike time histogram (10 ms bins); grey trace, instantaneous firing rate, as described in Materials and methods. (B) Raster plot of spikes recorded in 20 of the trials. (C) Time course of ocellar stimulation; LED intensity difference=(left LED output–right LED output);  $I_{\max}$ , max LED output.

determined for stimuli that changed at a number of different rates. The response to each stimulus was defined as the relative modulation,  $R_{\text{mod}}$ :

$$R_{\text{mod}} = \frac{R_{\text{max}} - R_{\text{min}}}{R_{\text{max}} + R_{\text{min}}}, \quad (3)$$

where  $R_{\text{max}}$  is the excitatory peak of the instantaneous firing rate and  $R_{\text{min}}$  the inhibitory trough (Fig. 7A).

The relationship between  $R_{\text{mod}}$  and the rate of change of stimulus intensity is shown in Fig. 7B. We normalised the data by assuming that the largest response was generated using a step stimulus, and scaling the data between this and the zero response value of  $R_{\text{mod}}$ . The zero response point was set by calculating  $R_{\text{mod}}$  for data recorded where no stimulus was presented. The response rises in proportion to the rate of change of intensity in the range 0–50  $I_{\text{max}} \text{ s}^{-1}$ , and tends to saturate for

higher values. The observation that a steeper slope elicits a stronger response modulation is to be expected, since a steeper slope implies a faster rotation of the head.

#### V1's response to ocellar stimulation is robust

How does V1 respond to excitation by both the ocelli and compound eyes, and is the ocellar input robust enough to be detected in the presence of powerful inputs from the compound eye? By stimulating the lateral ocelli while presenting a moving grating to the compound eye, we studied the time course and amplitude of the ocellar-mediated response over the full range of activity levels in V1. As before, the ocellar stimulus consisted of a train of step changes in intensity designed to mimic successive clockwise and anticlockwise roll rotations (cf. Fig. 8B, stimulus trace). For compound eye stimulation we presented a moving sinusoidal grating, whose contrast was varied to change the spike rate of V1 (Fig. 8C). The combination of ocellar and compound eye stimuli elicited the responses shown in Fig. 8A. The small peaks of ocellar-mediated responses are visible even at the highest spiking rates of V1 ( $\sim 300 \text{ spikes s}^{-1}$ ). The response to ocellar stimuli is therefore robust enough to be observed at all levels of V1's response range. The spike raster plots (Fig. 8D) show that the temporal coherence of ocellar-induced spikes was increased by raising V1's spike rate, and as mentioned above, is accompanied by a reduction in response latency. In the experiment shown in Fig. 8 the peak-response latency to the ocellar stimuli was reduced from approximately 18 ms to 13 ms.

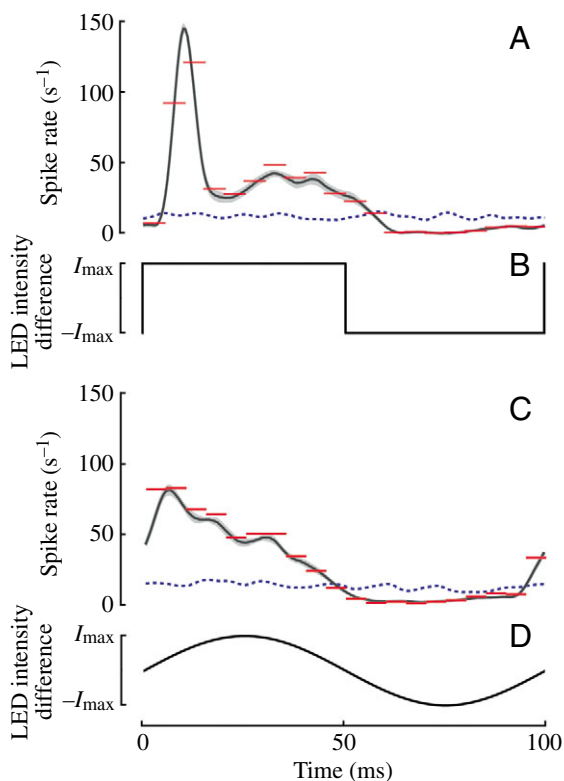
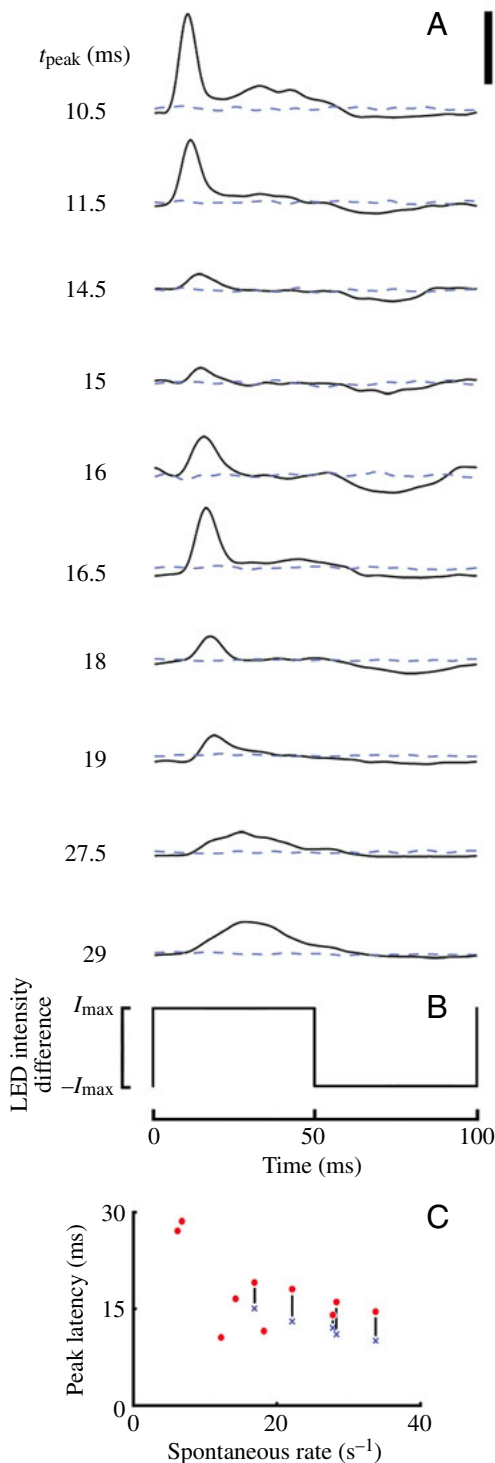


Fig. 5. The time course of the response of V1 neuron to a step change in ocellar light intensity (A,B), and a sinusoidal change (C,D). (A,C) Solid black lines: instantaneous firing rates averaged over 520 stimulus cycles; horizontal red lines: corresponding post-stimulus spike time histogram (5 ms bins); broken blue line: instantaneous firing rate of spontaneous activity, obtained during periods of zero stimulation between trials. (B,C) Time course of stimuli: LED intensity difference = (left LED output–right LED output);  $I_{\max}$ , max LED output. Stimuli were applied in 40 blocks of 15 consecutive cycles. The blocks were separated by 2.5 s. The first and last cycle of each block was discarded to give 520 cycles.

Fig. 8E,F shows, for two cells, the relationship between the absolute changes in spike rate due to ocellar stimuli and the spiking activity induced by the moving grating. This was found by subtracting the compound eye-only response from the combined stimuli response, at the time of each ocellar-mediated excitatory peak. To highlight a particular feature of these data, we applied a set of smoothing spline fits (black lines: Fig. 8E,F, see Materials and methods). These show that the maximum ocellar-induced excitation *and* inhibition occur at



similar spike rates,  $\sim 70$  spikes s<sup>-1</sup>, and the magnitude of the ocellar response tails-off slowly as the spike rate is further increased.

## Discussion

We have shown that the lobula plate tangential cell V1 responds to signals originating in the ocellar visual system. Three properties of the response to ocellar signals strongly suggest that the connection is synaptic, rather than neuromodulatory: (i) the short latency of post-stimulus spiking in V1 (Fig. 5), (ii) the high degree of temporal coherence of the first post-stimulus spike (Fig. 4), and (iii) the observation that the ocellar-mediated latency is reduced when V1's spike rate is increased as a result of compound eye input (Figs 6, 8). The response to ocellar input is dependent on the apparent direction of the stimulus; V1 was excited by changes in ocellar illumination that mimicked clockwise roll, and inhibited by changes that mimicked rotation in the opposite direction. Thus the ocellar component of V1's response appears to be tuned to rotation, similar to that shown for the compound eye component (Karmeier et al., 2003). The neurone's response increases with the rate at which light intensity changes at the ocelli (Fig. 7), implying that V1 might be able to code the angular velocity of the rotations sensed by the ocelli.

### Methodological limitations

Since the primary objective was to test whether the ocelli have any impact on LPTC activity, we did not set up our ocellar stimuli for an exhaustive analysis. We only stimulated the lateral ocelli and this limited the rotations mimicked by our stimuli to the anterior–posterior axis. Under normal conditions during a rotation about this axis, the frontal ocellus would also be constantly illuminated. Nonetheless, the qualitative demonstration of the interactions between the ocellar and compound eye visual systems we present here is convincing. Our aim in future experiments is to stimulate all three ocelli and quantify the integration of more realistic inputs from the two visual systems.

### Integrating inputs from compound eyes and ocelli

Though the visual system of the fly is among the best studied of all insect model systems, there is little previous evidence

Fig. 6. The time course and latencies of the responses of 10 V1 neurones to step ocellar stimuli. (A) Instantaneous firing rates from 10 neurones arranged according to the latency of peak activity,  $t_{\text{peak}}$ . Data were averaged over more than 100 trials for each animal, the scale bar shows 100 spikes s<sup>-1</sup>. Blue broken lines indicate the spontaneous firing rate. (B) Stimulus sequence presented in each trial; LED intensity difference=(left LED output–right LED output);  $I_{\text{max}}$ , max LED output. (C) The latency of peak activity plotted against spontaneous firing rate. Red dots: latency *versus* spontaneous rate for the 10 neurones shown in A; blue crosses: the reduced peak latencies recorded when five of these cells were driven at >250 spikes s<sup>-1</sup> by stimulating the compound eye. The vertical bars indicate a significant reduction of latency in each cell.

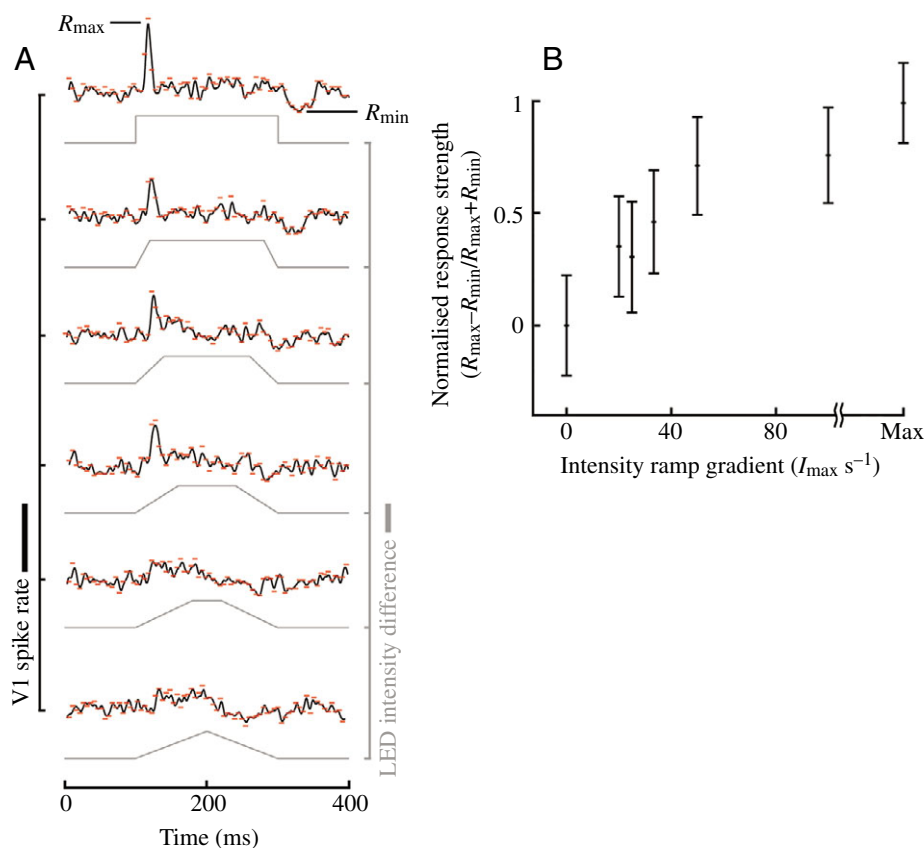


Fig. 7. The response of V1 neuron to ocellar stimuli that changed intensity at different rates. (A) V1 responses at six rates of change; black lines: instantaneous firing rates (see Materials and methods), scale bar, 50 spikes  $s^{-1}$ ; red lines: peristimulus spike histograms (5 ms bins); grey lines: time courses of the intensity changes, plotted as LED intensity difference=(left LED output–right LED output), scale bar,  $2I_{\max}$ . Stimuli ramped from  $-I_{\max}$  to  $I_{\max}$  and then back to  $-I_{\max}$ , where  $I_{\max}$ =max LED output. (B) The relative modulation,  $R_{\text{mod}}$  of V1 (see main text) plotted against the rate of change of ocellar intensity, expressed as  $I_{\max} s^{-1}$ . The data have been normalised to the range of responses between that elicited by a step stimulus (maximum  $R_{\text{mod}}$ ) and by zero stimulus (minimum, but non-zero  $R_{\text{mod}}$ ).

for the integration of compound eye and ocellar-mediated information in the optic lobes. Milde recorded the responses to ocellar and visual stimuli of several types of neurones in the protocerebrum of the honeybee (Milde, 1986; Milde, 1988). Both third-order ocellar neurones and interneurones originating in the lobula or medulla of the bee were found to respond to ocellar and compound eye stimulation, but in a somewhat erratic way. Consequently, the responses of these neurones were not fully characterised. In the locust, Simmons found that the descending contralateral movement detector (DCMD), a well-characterised visual interneurone thought to be involved in looming detection, responds to changes in light intensity at the median ocellus (Simmons, 1981). Simmons concluded that the function of ocellar input to the DCMD is to transiently boost the response of the cell to compound eye input when ocellar light levels suddenly decrease.

The situation in the blowfly lobula plate is more clear-cut. We already know that V1 is tuned to respond to the optic flow that is generated in the compound eye by rotation about a specific horizontal axis (Krapp et al., 2001), and we have discovered here that it also responds to ocellar stimuli that mimic similar rotations. We can now build on the knowledge

that V1 encodes visual information in a simple, explicable way to investigate two related sets of problems. We can investigate ocellar function by monitoring V1 activity induced by the ocelli, and we can study multisensory integration by measuring how this identified neurone integrates rotation-related signals from two different sets of sensors.

#### Ocellar-mediated motor responses

How important are the ocelli for gaze and flight stabilisation? Arguably the most complete picture so far is evident in locusts. Locust L-neurones were shown to have a fairly direct route, *via* descending neurones, to the flight motor system (Simmons, 2002) and are demonstrably important for flight steering (Taylor, 1981a; Taylor, 1981b). In dragonflies, there is strong behavioural evidence that similar pathways exist between ocellar neurones and neck muscles (Stange, 1981; Stange and Howard, 1979). The morphology of third-order ocellar neurones in the cockroach is similar to those in locusts, suggesting an analogous function (Mizunami, 1995a; Mizunami, 1995b).

In the blowfly, behavioural experiments investigating the phasic dorsal light response, which is mediated by the ocelli,

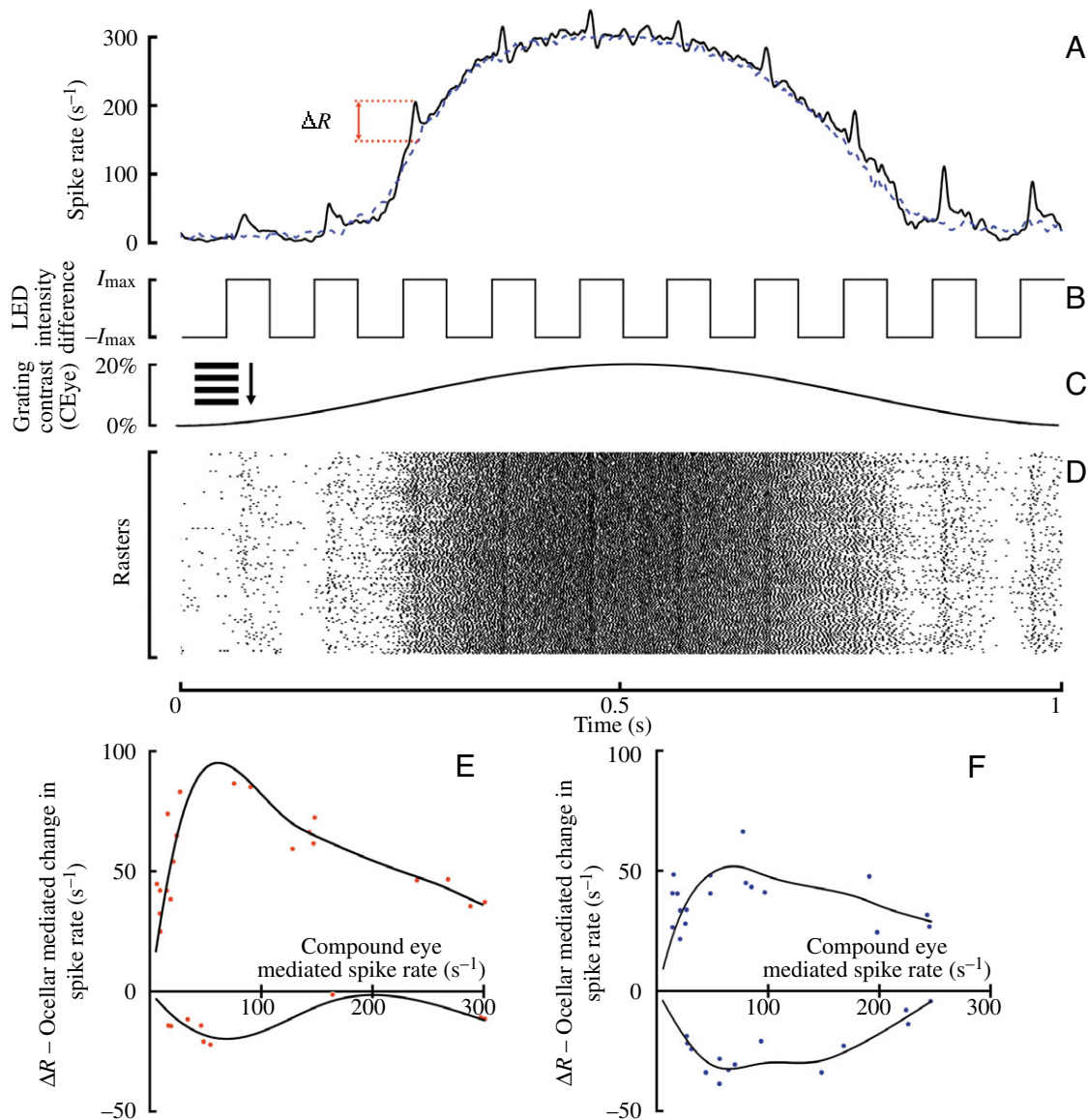


Fig. 8. The response of V1 neuron to combined stimulation of the ocelli and compound eye. (A) The instantaneous firing rate of V1 during stimulation of both the ocelli and compound eye (solid black line) and stimulation of the compound eye only (broken blue line). Data were averaged over 155 repetitions of the stimulus from a single animal. (B) Time course of ocellar stimulation. (C) Time course of the contrast of the compound eye stimulation. The data in A were obtained using a contrast increase of 0% to 20%. (D) The full set of 155 spike train rasters obtained during combined stimulation. (E) The peak ocellar-mediated change in V1 spike rate,  $\Delta R$ , plotted against the corresponding compound eye-only mediated value, at the time of each peak. Positive y-axis values therefore indicate ocellar-mediated excitation, whereas negative values indicate ocellar-mediated inhibition. To obtain enough data points, both the curves shown in C (0–10% and 0–20%) were used to stimulate the compound eyes. (F) Data from another animal (188 stimulus repetitions), presented in the same way as in E. Black lines in E and F are interpolant smoothing splines, each obtained using the same smoothing parameter (see Materials and methods).

showed only small amplitude compensatory head roll movements (Schuppe and Hengstenberg, 1993) in response to differential illumination of the lateral ocelli. The light level in these experiments, however, was only changed in one ocellus, while the other two were occluded. The same experimental paradigm was used in experiments to obtain the angular velocity dependence of compensatory head roll movements (Hengstenberg, 1988) for compound eye-mediated reflexes. It was found that the response to directional motion mediated by the compound eye was maximal at  $\sim 70^\circ \text{ s}^{-1}$ , but that the dorsal

light response, which also involves the ocelli, extended with high gain up to angular velocities of  $\sim 500^\circ \text{ s}^{-1}$ . The conclusion of this behavioural work was that the ocelli act in conjunction with the compound eyes and mechanosensory halteres to detect and monitor self-rotations. The sensitivity of the ocellar system to changes in attitude during flight lies within an angular velocity range in between that of the compound eyes and the mechanosensory halteres (Hengstenberg, 1993). Our recordings from V1 show that the LPTCs could play an important role in combining information from ocelli and

compound eyes, supplying descending neurones and motor neurones with appropriate signals for attitude control.

#### *What neural pathway conveys ocellar information to V1?*

It is likely that a fast neural circuit connects the ocelli to V1, because the short response delays (10–20 ms) seen in our experiments exclude neuromodulatory effects. Because of the limitations of extracellular recordings, we were not able to identify synaptic inputs to V1, but there is circumstantial evidence for an interesting pattern of neuronal connectivity. During the course of the ocellar-V1 experiments, several recordings were also obtained from V2, another heterolateral LPTC (Hausen, 1993). Like V1, this cell also codes for self-rotation about a horizontal axis but, unlike V1, it did not respond to stimulation of the lateral ocelli. This difference may be explained by examining the function and morphology of the two cells. V1 and V2 are similar in that both cells send an axon from their dendritic input regions to the lobula plate on the opposite side of the brain, where telodendritic output arborisations are formed (Hausen, 1993; Krapp et al., 2001; Kurtz et al., 2001; Warzecha et al., 2003). V2, however, most likely receives direct retinotopic input from the compound eyes (Krapp, 1995), whereas V1 integrates the outputs of another set of LPTCs, the VS cells (primarily VS1–3) (Kurtz et al., 2001). It is possible then, that the reason we see ocellar-mediated activity changes in V1 but not in V2, is that the ocelli drive VS cells 1–3, which are presynaptic to V1. The connection between the ocellar system and the VS cells could be either directly from ocellar L-neurones, or *via* descending neurones, which, through electrical synapses, influence the membrane potential of VS1–VS3 (Strausfeld and Bassemir, 1985). Recent work on the VS–V1 synapse would seem to support the L-neurone–VS–V1 route. The relationship between presynaptic (VS-cell) membrane potential and postsynaptic (V1) spike rate is almost linear (Kurtz et al., 2001; Warzecha et al., 2003), but only above a certain level of pre-synaptic depolarisation. This fits with the observation (Fig. 8B,C) that the largest responses to ocellar inputs were observed when the activity level of V1 was raised slightly above baseline by compound eye stimulation. In any case, to identify the pathway mediating ocellar-induced activity changes in V1 further experiments are required, ideally monitoring the ocellar nerve activity while recording intracellularly and extracellularly from VS cells and V1, respectively.

#### *Why convey sensory information from the ocelli to the lobula plate?*

Because the VS tangential cells are matched filters for self-rotation, they are ideal targets for inputs from ocellar L-neurones. By integrating the appropriate combination of ocellar L-neurone outputs, each tangential cell could include ocellar-mediated information on rotations in a way that matches its preferred rotation axis. Our data suggest that this may be the case for the V1 cell, and thus for the inputting VS-cells, because the ocellar-mediated input to V1 conveys information about turns that is compatible with the neurone's preferred axis of rotation.

The compound eye stimulus that most strongly activates V1 corresponds to the optic flow generated by a rotation of the fly about a horizontal axis intermediate between pitch and roll (Fig. 2). For the roll component this is a clockwise rotation that decreases the light level in the right ocellus and increases it in the left ocellus. Mimicking such an illumination pattern increased the V1 spiking activity whereas the opposite pattern of illumination resulted in a reduced spike rate. The integration of ocellar inputs at the level of LPTCs could very well be advantageous in the context of sensorimotor transformation: it reduces the need for ocellar-specific interneurones to transform information obtained in sensory coordinates into the signals required by the motor system for attitude control. A similar simplification of the sensorimotor transformation has recently been suggested in the gaze stabilization system of the blowfly (Huston, 2005; S. Huston and H.G.K., unpublished data).

Any functional integration of ocellar information at the level of the LPTCs would be meaningless if a major advantage of the ocellar system – its speed – was negated. Our measurements of the latency of ocellar-mediated V1 modulations suggest that this advantage is maintained. We observed a median (over ten cells) time-to-peak latency of ~16 ms, with a minimum latency in one cell of 10.5 ms, whereas the response latency in tangential neurones to compound eye stimulation is about 25 ms (Warzecha and Egelhaaf, 2000). Our estimates of the latency will be slightly conservative in comparison with the study mentioned in the previous sentence. This is because we looked at peak latency, which is essentially the mean position of the first post-stimulus spike, whereas Warzecha and Egelhaaf (Warzecha and Egelhaaf, 2000) based their estimates around discrimination of the neuronal signal from background noise. The precise latency advantage of ocellar responses must be confirmed using a single stimulus that drives both the ocelli and the compound eye simultaneously with equivalent light intensities.

#### *Multimodal integration in the lobula plate*

The arguments presented above suggest how ocellar signals could be integrated in the lobula plate to produce faster motor responses, by using the VS cells as ready-tuned conduits to the motor system. There is preliminary evidence that neurones in the fly lobula plate integrate other forms of sensory input that are useful for controlling flight. Spiking in LPTCs can be modulated by wind stimuli applied to the antennae, and by mechanical stimulation of the abdomen (S. L. Maddess and S. Huston, unpublished observations). Further investigation of these interactions, along with a quantitative description of the integration of ocellar and compound eye-mediated signals in V1 and VS neurones, promise considerable insight into the neural principles of multisensory integration. Because the visual response properties of LPTCs are exceptionally well characterised, such studies may be able to identify some of the synergies that occur when different sensory systems independently encode the same parameter to control a specific behaviour and also show how these synergies are implemented in circuits composed of identified neurones.

This work was supported by a PhD studentship from the BBSRC to M.M.P. and a USAF grant to H.G.K.

### References

- Fayyazuddin, A. and Dickinson, M. H. (1999). Convergent mechanosensory input structures the firing phase of a steering motor neuron in the blowfly, *Calliphora*. *J. Neurophysiol.* **82**, 1916-1926.
- Fraenkel, G. and Pringle, J. W. S. (1938). Halteres of flies as gyroscopic organs of equilibrium. *Nature* **141**, 919-921.
- Franceschini, N. (1975). Sampling of the visual environment by the compound eye of the fly: fundamentals and applications. In *Photoreceptor Optics* (ed. A. W. Snyder and R. Menzel), pp. 98-125. New York: Springer.
- Gabbiani, F., Krapp, H. G. and Laurent, G. (1999). Computation of object approach by a wide-field, motion-sensitive neuron. *J. Neurosci.* **19**, 1122-1141.
- Haag, J., Denk, W. and Borst, A. (2004). Fly motion vision is based on Reichardt detectors regardless of the signal-to-noise ratio. *Proc. Natl. Acad. Sci. USA* **101**, 16333-16338.
- Hausen, K. (1993). Decoding of retinal image flow in insects. *Rev. Oculomot. Res.* **5**, 203-235.
- Heide, G. (1974). The influence of wingbeat synchronous feedback on the motor output systems in flies. *Z. Naturforsch. C J. Biosci.* **29**, 739-744.
- Hengstenberg, R. (1988). Mechanosensory control of compensatory head roll during flight in the blowfly *Calliphora erythrocephala* Meig. *J. Comp. Physiol. A Sens. Neural Behav. Physiol.* **163**, 151-165.
- Hengstenberg, R. (1993). Multisensory control in insect oculomotor systems. *Rev. Oculomot. Res.* **5**, 285-298.
- Huston, S. (2005). *Neural Basis of a Visuo-Motor Transformation in the Fly*. PhD thesis, Cambridge University, Cambridge, UK.
- Karmeier, K., Krapp, H. G. and Egelhaaf, M. (2003). Robustness of the tuning of fly visual interneurons to rotatory optic flow. *J. Neurophysiol.* **90**, 1626-1634.
- Keil, T. A. (1997). Functional morphology of insect mechanoreceptors. *Microsc. Res. Tech.* **39**, 506-531.
- Kirschfeld, K., Feiler, R. and Vogt, K. (1988). Evidence for a sensitizing pigment in the ocellar photoreceptors of the blowfly (*Musca*, *Calliphora*). *J. Comp. Physiol. A Sens. Neural Behav. Physiol.* **163**, 421-423.
- Krapp, H. G. (1995). *Repräsentation von eigenbewegungen der schmeißfliege Calliphora erythrocephala in VS-neuronen des dritten visuellen neuropils*. PhD thesis, Universität Tübingen, Tübingen, Germany.
- Krapp, H. G. (2000). Neuronal matched filters for optic flow processing in flying insects. *Int. Rev. Neurobiol.* **44**, 93-120.
- Krapp, H. G. and Hengstenberg, R. (1996). Estimation of self-motion by optic flow processing in single visual interneurons. *Nature* **384**, 463-466.
- Krapp, H. G., Hengstenberg, B. and Hengstenberg, R. (1998). Dendritic structure and receptive-field organization of optic flow processing interneurons in the fly. *J. Neurophysiol.* **79**, 1902-1917.
- Krapp, H. G., Hengstenberg, R. and Egelhaaf, M. (2001). Binocular contributions to optic flow processing in the fly visual system. *J. Neurophysiol.* **85**, 724-734.
- Kurtz, R., Warzecha, A. K. and Egelhaaf, M. (2001). Transfer of visual motion information via graded synapses operates linearly in the natural activity range. *J. Neurosci.* **21**, 6957-6966.
- Milde, J. J. (1986). Characteristics of interneurons in the ocellar system of the honeybee. *Exp. Biol.* **46**, 1-9.
- Milde, J. J. (1988). Visual responses of interneurons in the posterior median protocerebrum and the central complex of the honeybee *Apis mellifera*. *J. Insect Physiol.* **34**, 427-436.
- Mizunami, M. (1995a). Morphology of higher-order ocellar interneurons in the cockroach brain. *J. Comp. Neurol.* **362**, 293-304.
- Mizunami, M. (1995b). Neural organization of ocellar pathways in the cockroach brain. *J. Comp. Neurol.* **352**, 458-468.
- Nalbach, G. (1993). The halteres of the blowfly *Calliphora*. 1. Kinematics and dynamics. *J. Comp. Physiol. A Sens. Neural Behav. Physiol.* **173**, 293-300.
- Nalbach, G. and Hengstenberg, R. (1994). The halteres of the blowfly *Calliphora*. 2. 3-dimensional organization of compensatory reactions to real and simulated rotations. *J. Comp. Physiol. A Sens. Neural Behav. Physiol.* **175**, 695-708.
- Nässel, D. R. and Hagberg, M. (1985). Ocellar interneurons in the blowfly *Calliphora erythrocephala*: morphology and central projections. *Cell Tissue Res.* **242**, 417-426.
- Reichardt, W. (1987). Evaluation of optical motion information by movement detectors. *J. Comp. Physiol. A Sens. Neural Behav. Physiol.* **161**, 533-547.
- Schuppe, H. and Hengstenberg, R. (1993). Optical-properties of the ocelli of *Calliphora erythrocephala* and their role in the dorsal light response. *J. Comp. Physiol. A Sens. Neural Behav. Physiol.* **173**, 143-149.
- Sherman, A. and Dickinson, M. H. (2003). A comparison of visual and haltere-mediated equilibrium reflexes in the fruit fly *Drosophila melanogaster*. *J. Exp. Biol.* **206**, 295-302.
- Simmons, P. J. (1981). Ocellar excitation of the Dcmd: an identified locust interneurone. *J. Exp. Biol.* **91**, 355-359.
- Simmons, P. J. (1999). The performance of synapses that convey discrete graded potentials in an insect visual pathway. *J. Neurosci.* **19**, 10584-10594.
- Simmons, P. J. (2002). Signal processing in a simple visual system: the locust ocellar system and its synapses. *Microsc. Res. Tech.* **56**, 270-280.
- Simmons, P. J., Jian, S. and Rind, F. C. (1994). Characterization of large 2nd order ocellar neurons of the blowfly *Calliphora erythrocephala*. *J. Exp. Biol.* **191**, 231-245.
- Stange, G. (1981). The ocellar component of flight equilibrium control in dragonflies. *J. Comp. Physiol.* **141**, 335-347.
- Stange, G. and Howard, J. (1979). Ocellar dorsal light response in a dragonfly. *J. Exp. Biol.* **83**, 351-355.
- Stange, G., Stowe, S., Chahl, J. S. and Massaro, A. (2002). Anisotropic imaging in the dragonfly median ocellus: a matched filter for horizon detection. *J. Comp. Physiol. A Neuroethol. Sens. Neural Behav. Physiol.* **188**, 455-467.
- Strausfeld, N. J. (1976). *Atlas of an Insect Brain*. Berlin, New York: Springer-Verlag.
- Strausfeld, N. J. and Bassemir, U. K. (1985). Lobula plate and ocellar interneurons converge onto a cluster of descending neurons leading to neck and leg motor neuropil in *Calliphora erythrocephala*. *Cell Tissue Res.* **240**, 617-640.
- Strausfeld, N. J. and Gronenberg, W. (1990). Descending neurons supplying the neck and flight motor of diptera – organization and neuroanatomical relationships with visual pathways. *J. Comp. Neurol.* **302**, 954-972.
- Taylor, C. P. (1981a). Contribution of compound eyes and ocelli to steering of locusts in flight. 1. Behavioral analysis. *J. Exp. Biol.* **93**, 1-18.
- Taylor, C. P. (1981b). Contribution of compound eyes and ocelli to steering of locusts in flight. 2. Timing changes in flight motor units. *J. Exp. Biol.* **93**, 19-31.
- Warzecha, A. and Egelhaaf, M. (2000). Response latency of a motion-sensitive neuron in the fly visual system: dependence on stimulus parameters and physiological conditions. *Vision Res.* **40**, 2973-2983.
- Warzecha, A. K., Kurtz, R. and Egelhaaf, M. (2003). Synaptic transfer of dynamic motion information between identified neurons in the visual system of the blowfly. *Neuroscience* **119**, 1103-1112.
- Wilson, M. (1978a). Functional organization of locust ocelli. *J. Comp. Physiol.* **124**, 297-316.
- Wilson, M. (1978b). Generation of graded potential signals in 2nd order cells of locust ocellus. *J. Comp. Physiol.* **124**, 317-331.